

Effects of Co-Doping on Dielectric and Electrical Responses of $\text{CaCu}_3\text{Ti}_{4-x}(\text{Nb}_{1/2}\text{In}_{1/2})_x\text{O}_{12}$ Ceramics

Jakkree Boonlakhorn¹, Pinit Kidkhunthod², and Prasit Thongbai^{1,*}

¹Integrated Nanotechnology Research Center (INRC), Department of Physics, Faculty of Science, Khon Kaen University, Khon Kaen 40002, Thailand

²Synchrotron Light Research Institute (Public Organization), 111 University Avenue, Muang District, Nakhon Ratchasima 30000, Thailand

Email: pthongbai@kku.ac.th

Abstract. In this work, $\text{CaCu}_3\text{Ti}_{4-x}(\text{Nb}_{1/2}\text{In}_{1/2})_x\text{O}_{12}$ ceramics, $x = 0, 0.025, 0.05, 0.10,$ and $0.20,$ were prepared using a conventional solid state reaction method. Their crystal structure, microstructure, dielectric, and electrical properties were systematically investigated. A primary phase of $\text{CaCu}_3\text{Ti}_4\text{O}_{12}$ ceramic was clearly observed in all samples. The average grain size of $\text{CaCu}_3\text{Ti}_4\text{O}_{12}$ was decreased by $(\text{Nb}^{5+}, \text{In}^{3+})$ doping. The dielectric permittivity of $\text{CaCu}_3\text{Ti}_{4-x}(\text{Nb}_{1/2}\text{In}_{1/2})_x\text{O}_{12}$ ceramics was slightly dependent on frequency as the co-dopant concentration increased, which was due to a decrease in its grain size. Their dielectric behavior can be well described by the internal barrier layer capacitor (IBLC) model based on interfacial polarization at grain boundaries. The grain boundary resistance and potential barrier height at the grain boundary of $\text{CaCu}_3\text{Ti}_4\text{O}_{12}$ were reduced by co-doping with $(\text{Nb}^{5+}, \text{In}^{3+})$ ions, resulting in an enhancement of DC conductivity and the related dielectric loss tangent.

1. Introduction

A dielectric material is one of many classes of materials that has been widely studied for use in electronic applications, especially for capacitors [1-3]. Recently, the giant dielectric properties of $\text{CaCu}_3\text{Ti}_4\text{O}_{12}$ ceramics (CCTO) have been reported. Most researchers believed that either the intrinsic or the extrinsic effect is the origin of the giant dielectric behavior of CCTO ceramics [2, 4-6]. Recently, an internal barrier layer capacitor (IBLC) model has been widely and reasonably used to explain the high dielectric permittivity (ϵ') of CCTO ceramics [2-4, 6]. This is because CCTO consists of semiconducting grains and insulating grain boundaries (GBs). The different electrical properties of the grains and GBs were due to variations in their chemical composition [7, 8]. According to the IBLC model, the grain size and thickness of GBs are very important parameters contributing to the giant dielectric response in CCTO ceramics. The loss factor ($\tan\delta$) is directly proportional to the mean grain size, which is inversely

proportional to the number of GB layers. Therefore, effects of grain size and thickness of GBs on the dielectric properties of CCTO should be systematically investigated.

To study these factors, variation of electrical properties of the grains and GBs as a result of incorporation of doping ions has been investigated to confirm the change in dielectric properties [2, 3, 6]. Doping CCTO with metal ions was therefore selected as a suitable strategy to test this hypothesis. In this work, Nb^{5+} and In^{3+} ions were selected as co-dopants to be substituted into Ti^{4+} sites of the CCTO structure. X-ray Diffractometry (PANalytical, EMPYREAN), scanning electron microscopy (SEM; SEC, SNE-4500M), and impedance analysis (KEYSIGHT E4990A) were used to characterize and study the effects of (Nb^{5+} , In^{3+}) co-doping on the crystalline structure, microstructure, dielectric and electrical properties of $\text{CaCu}_3\text{Ti}_{4-x}(\text{Nb}_{1/2}\text{In}_{1/2})_x\text{O}_{12}$ ceramics. The experimental results are discussed in detail.

2. Experimental procedure

$\text{CaCu}_3\text{Ti}_{4-x}(\text{Nb}_{1/2}\text{In}_{1/2})_x\text{O}_{12}$ ceramics, where $x = 0, 0.025, 0.05, 0.10,$ and 0.20 , were prepared via a solid state reaction method. The raw materials consisted of CaCO_3 , CuO , TiO_2 , Nb_2O_5 , In_2O_3 , and $\text{C}_2\text{H}_5\text{OH}$. First, stoichiometric amounts of all starting raw materials for each chemical formulation were placed in plastic bottles and mixed in a ball mill for 24 h. Second, the mixed raw materials were poured into beakers and dried at $100\text{ }^\circ\text{C}$ for 24 h. Third, the dried precursors were ground and calcined at $850\text{ }^\circ\text{C}$ for 12 h. All the calcined powders were pressed in uniaxial compression at $\sim 200\text{ MPa}$ into pellet shaped specimens, 9.5 mm in diameter and $\sim 1.2\text{ mm}$ in thickness. Finally, all the green bodies were sintered at $1090\text{ }^\circ\text{C}$ for 18 h. The $\text{CaCu}_3\text{Ti}_{4-x}(\text{Nb}_{1/2}\text{In}_{1/2})_x\text{O}_{12}$ ceramics, $x = 0, 0.025, 0.05, 0.10,$ and 0.20 are referred to as the CCTO, NI025, NI05, NI10, and NI20 ceramics, respectively.

3. Results and discussion

Figs. 1(a–b) show XRD patterns of the CCTO, NI025, NI05, NI10, and NI20 ceramics and a Rietveld profile fit of the NI025 ceramic. The XRD patterns confirmed the formation of a primary phase of CCTO (JCPDS 75–2188). No impurity phase was observed in any of the XRD patterns. Lattice parameters of the CCTO, NI025, NI05, NI10, and NI20 ceramics were found to be 7.393(5), 7.395(6), 7.399(2), 7.405(6), and 7.418(6) Å, respectively. The a value of CCTO slightly increased with increasing co-dopant concentration. This may be due to the larger ionic radii of the co-dopants (In^{3+} , Nb^{5+}) ions than the Ti^{4+} host ion. As shown in Fig. 2, the mean grain size of CCTO was decreased by doping with ($\text{Nb}^{5+}+\text{In}^{3+}$). Strong suppression of grain growth in (Nb^{5+} , In^{3+}) co-doped CCTO ceramics was also caused by the smaller ionic radii of the co-dopants than the Ti^{4+} host ions, which can produce lattice strain energy. The initial segregation of In^{3+} and Nb^{5+} dopants at the GB can reduce the driving force for

motion of the GB during sintering, resulting in a decrease in the mean grain size compared to that of the un-doped CCTO ceramic [3].

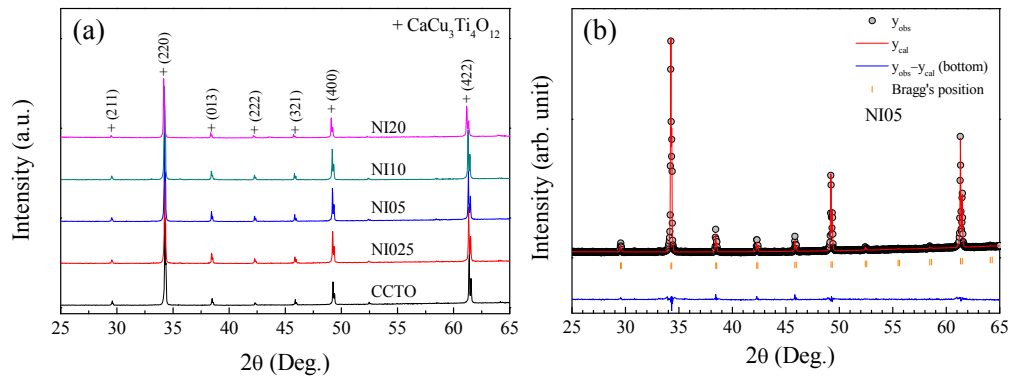


Figure 1 (a) XRD patterns of the CCTO, NI025, NI05, NI10, and NI20 ceramics and (b) Rietveld profile fit of the NI05 ceramic.

The frequency dependence of the CCTO, NI025, NI05, NI10, and NI20 ceramics at 30 °C is demonstrated in Fig. 3 (a). ϵ' of CCTO at a mid–high frequency range decreased with increasing dopant concentration. This is very consistent with the observed decrease in grain size. Clearly, when x was increased, a significant increase in $\tan\delta$ (inset of Fig. 3(a)) was observed. This very closely correspond to an increase in the ϵ' value due to an increase in DC conduction in a low frequency range. As shown in Fig. 3(b) and its inset, the step-like decrease in ϵ' , which is suggested to be a dielectric relaxation behavior, significantly shifted to higher frequencies when temperature was significantly increased. This indicates a thermally activated dielectric relaxation behavior.

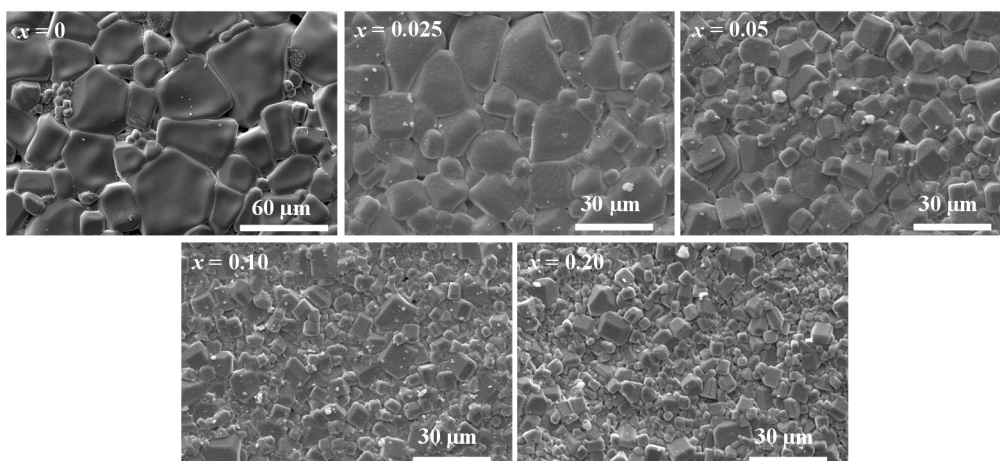


Figure 2 Surface morphologies of $\text{CaCu}_3\text{Ti}_{4-x}(\text{Nb}_{1/2}\text{In}_{1/2})_x\text{O}_{12}$ ceramics with $x = 0, 0.025, 0.05, 0.10,$ and 0.20 .

As illustrated in Fig. 4 and its insets, a large semicircular arc and nonzero intercept on the Z' axis are observed, indicating the electrical responses of the insulating GBs and semiconducting grains, respectively. Thus, the significant increase in $\tan\delta$ can be considered to originate from the reduction in the GB resistance (R_{gb}). Conduction activation energies of GBs (E_{gb}) were calculated from the variation of R_{gb} values at different temperatures. The E_{gb} values were found to be 0.698, 0.586, 0.482, 0.395, and 0.340 eV for the CCTO, NI025, NI05, NI10, and NI20 ceramics, respectively. This result indicates a plausible relationship between $\tan\delta$, R_{gb} , and E_{gb} . Moreover, both the mean grain size and grain resistance (R_g) have a strong influence on the value of ϵ' . The relationship between the dielectric properties and the R_{gb} , R_g , and microstructure of $\text{CaCu}_3\text{Ti}_{4-x}(\text{Nb}_{1/2}\text{In}_{1/2})_x\text{O}_{12}$ ceramics is likely to those observed by other researchers [2-4, 6, 9].

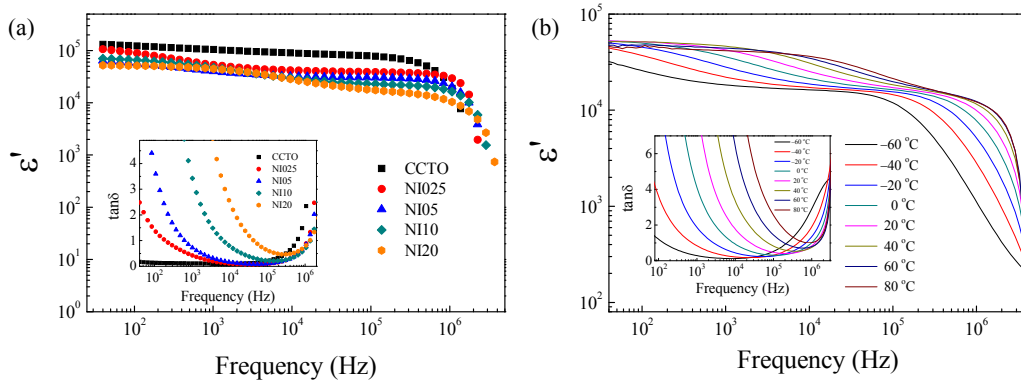


Figure 3 (a) Frequency dependence of ϵ' for CCTO, NI025, NI05, NI10, and NI20 ceramics at 30 °C; inset shows $\tan\delta$ as a function of frequency. (b) Frequency dependence of ϵ' at different temperatures for the NI20 ceramic; inset demonstrates $\tan\delta$ as a function of temperature.

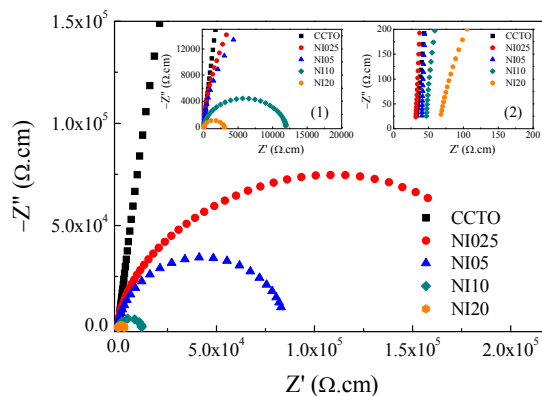


Figure 4 Impedance complex Z^* plots at 30 °C for the CCTO, NI025, NI05, NI10, and NI20 ceramics. Inset (1) shows an enlarged scale and (2) shows a high frequency Z^* plot.

4. Conclusion

A primary phase of CCTO was achieved in all samples. Their mean grain sizes were significantly reduced by co-doping with (Nb^{5+} , In^{3+}). The variation of ϵ' was very consistent with changes in their microstructure and R_g values. At the same time, $\tan\delta$ values corresponded with their R_{gb} values.

5. Acknowledgement

This work was financially supported by the Integrated Nanotechnology Research Center (INRC), Khon Kaen University. J. Boonlakhorn would like to thank the Graduate School, Khon Kaen University for his PhD scholarship (Grant Number 581T211).

6. References

- [1] Homes C C, Vogt T, Shapiro S M, Wakimoto S and Ramirez A P 2001 *Science* **293** 673-6
- [2] Ni L and Chen X M 2009 *Solid State Commun.* **149** 379-83
- [3] Boonlakhorn J, Thongbai P, Putasaeng B, Yamwong T and Maensiri S 2014 *J. Alloys Compd.* **612** 103-9
- [4] Sinclair D C, Adams T B, Morrison F D and West A R 2002 *Appl. Phys. Lett.* **80** 2153
- [5] Ni L and Chen X M 2010 *J. Am. Ceram. Soc.* **93** 184-9
- [6] Schmidt R, Stennett M C, Hyatt N C, Pokorny J, Prado-Gonjal J, Li M and Sinclair D C 2012 *J. Eur. Ceram. Soc.* **32** 3313-23
- [7] Adams T B, Sinclair D C and West A R 2006 *J. Am. Ceram. Soc.* **89** 3129-35
- [8] Chung S-Y, Kim I-D and Kang S-J L 2004 *Nat. Mater.* **3** 774-8
- [9] Sun L, Zhang R, Wang Z, Cao E, Zhang Y and Ju L 2016 *RSC Adv.* **6** 55984-9